Proc. Natl. Acad. Sci. USA
Vol. 89, pp. 10336–10340, November 1992
Biochemistry

Quadruplex structure of $d(G_3T_4G_3)$ stabilized by K^+ or Na^+ is an asymmetric hairpin dimer

P. V. SCARIA*, STEVEN J. SHIRE†, AND RICHARD H. SHAFER*‡

*Department of Pharmaceutical Chemistry, School of Pharmacy, University of California, San Francisco, CA 94143; and †Department of Pharmaceutical Research and Development, Genentech, Inc., South San Francisco, CA 94080

Communicated by I. Tinoco, Jr., July 1, 1992

ABSTRACT **The ends of chromosomes contain repeats of guanine-rich sequences that can assume highly compact conformations and are presumed necessary for their biological role in chromosomal stabilization and association. We have investigated the conformational behavior of $d(G_3T_4G_3)$ as a function of the addition of either KCl or NaCl, in the concentration range of 50–200 mM, by using a spectrum of physical techniques and conclude that these salts induce a quadruplex species composed of two strands, each in a hairpin conformation. When salt is added, a large positive signal appears near 290 nm in the CD spectra. UV thermal denaturation curves show a single concentration-dependent transition and provide data for quantitating the thermodynamics of quadruplex formation. In electrophoresis experiments, the quadruplex structure migrates as a single species and more rapidly than the unstructured single strand. NMR spectra in the presence of KCl or NaCl indicate that the structure formed is asymmetric. Equilibrium ultracentrifugation studies confirm that these quadruplexes are composed of two strands of $d(G_3T_4G_3)$. Possible models for this structure are discussed.**

The ends of chromosomes, termed telomeres, contain a single-stranded 3′ overhang composed of repeats of guanine-rich sequences, such as $d(G_4T_4)$ and $d(G_4T_2)$. Telomeric DNA sequences can take on highly compact conformations that are presumed necessary for their biological role in chromosomal stabilization and association (1–3). Such structures often entail hairpin or fold-back forms involving one or two strands of G-rich DNA (4). Hastie and Allshire (5) have discussed the possible role of quadruplex structures in recombination, and Sen and Gilbert (6) have described four-stranded guanine-rich structures (G4 DNA) formed by several telomeric sequences. Furthermore, there is evidence that G-rich runs in immunoglobulin switch regions may form four-stranded quadruplex structures (7). Guanine-rich sequences have also been found in gene promoter regions (8, 9).

In all of these unusual forms, the fundamental structural unit—the guanine quartet—is composed of four guanines arrayed in a square planar configuration. Each guanine interacts with each of the two adjacent guanines through two Hoogsteen-like hydrogen bonds. The simplest system potentially capable of guanine quartet formation consists of guanine nucleosides or nucleotides, solutions of which have long been known to form gels (10). Recently, Lipanov *et al.* (11) have obtained crystals of $Na_2$5′-GMP. Preliminary x-ray analysis has revealed a helical pattern that can be interpreted in terms of a quadruple helix made up of three guanine quartets. Earlier reports have also appeared describing parallel four-stranded structures for poly(G) and poly(I) (12). In the last 5 years, several telomeric sequences have been studied using physical and structural methods (13–18). Henderson *et al.* (15) have examined a variety of sequences with enhanced electrophoretic mobility that exhibited low-field exchangeable protons in the NMR spectra, indicating the presence of G·G base pairing. In addition, their two-dimensional NMR data provided evidence for the presence of both *syn* and *anti* conformations for the nucleosides. Jin *et al.* (16) have described several quadruplexes composed of deoxynonanucleotides. NMR evidence was also presented for Hoogsteen-like interactions and thermodynamic measurements indicated that these were four-stranded structures.

Hardin *et al.* (17) have investigated several telomeric sequences using NMR, CD, and UV thermal denaturation measurements. They observed that hairpin and four-stranded structures were preferentially stabilized by different cations. Wang *et al.* (18, 19) have carried out two-dimensional NMR studies on several deoxynonanucleotides and demonstrated the presence of Hoogsteen interactions involving both imino and amino protons of guanine along with alternating *syn* and *anti* conformations within each strand. Their NMR data were consistent with either a four-stranded structure or a dimeric hairpin structure, but unequivocal discrimination between these forms was not possible.

Two studies have appeared very recently on the sequence $d(G_4T_4G_4)$, derived from the G_4T_4 repeat from *Oxytricha*. The reported x-ray diffraction study of a telomeric sequence, carried out on a sample crystallized from a solution containing KCl, $MgCl_2$, and spermine, led to a symmetric dimer hairpin structure in which the thymine loops lie at opposite ends, with the guanine quartets at the center (20). The planes containing the two loops are parallel to each other in this structure. In contrast to this arrangement, NMR analysis of the same sequence, in NaCl solution, resulted in a symmetric dimeric hairpin structure in which the planes of the two thymine loops are mutually perpendicular (21).

In this report, we describe an asymmetric quadruplex structure for $d(G_3T_4G_3)$ induced by the presence of either KCl or NaCl in the concentration range of 50–200 mM. Both polyacrylamide gel and capillary electrophoresis data indicate a single fast-migrating species in the presence of either salt. UV thermal denaturation studies also reveal a single transition and yield quantitative results for the thermodynamic stability of this structure. CD spectra show a pronounced positive band near 290 nm, and ^1H NMR spectra show the presence of 12 imino protons, along with a doubling of the aromatic peaks. Finally, equilibrium analytical ultracentrifugation data demonstrate that these structures are composed of two strands.

MATERIALS AND METHODS

Chemicals and Oligodeoxynucleotides. The oligodeoxynucleotide $d(G_3T_4G_3)$, a generous gift from Corey Levenson of Cetus, was synthesized by the cyanoethylphosphoramidite method on a Milligen/Biosearch 8800 DNA synthesizer. The anion-exchange HPLC purified oligomer was then dialyzed

The publication costs of this article were defrayed in part by page charge payment. This article must therefore be hereby marked "*advertisement*" in accordance with 18 U.S.C. §1734 solely to indicate this fact.

‡To whom reprint requests should be addressed.

extensively against 1 mM sodium cacodylate. Purity of the resulting sample was checked by polyacrylamide gel electrophoresis, capillary electrophoresis, and ^{1}H NMR. The molar extinction coefficient of the oligomer was determined by phosphate analysis (22) and was found to be 9900 cm^{-1}·(mol base per liter)$^{-1}$ at 256 nm. ^2H_2O was purchased from Aldrich and all the other reagents and chemicals were obtained from Sigma. Experiments were carried out with samples dialyzed against either 10 or 25 mM Tris·HCl (pH 7.5) to which various amounts of KCl or NaCl were added, as indicated. In all experiments, samples were heated at 75°C for ≈4 min and slowly cooled to room temperature after each addition of salt.

UV Absorbance Studies. Spectrophotometric experiments were carried out on a Gilford 2600 spectrophotometer, with temperature controlled by a Gilford 2527 thermoprogrammer. Thermal denaturation profiles were measured at a heating rate of 0.25°C/min with detection at 272 nm. Based on the results from our other experiments, we have assumed a bimolecular association of $d(G_3T_4G_3)$ strands to form the quadruplex structure, in an all-or-none fashion. The equilibrium can be written as 2 $d(G_3T_4G_3) \rightarrow d(G_3T_4G_3)_2$. Since this equilibrium is formally identical to that for duplex formation from self-complementary strands, we have used the equation derived for that equilibrium in evaluating the thermodynamic parameters for the quadruplex formation (23). Accordingly,

$$\frac{1}{T_{max}} = \frac{R}{\Delta H^\circ} \ln C_T + \frac{\Delta S^\circ + 0.505R}{\Delta H^\circ},$$

where T_{max} is the temperature corresponding to the maximum in the derivative plot [(dA/dT) vs. T] of the UV melting profile, C_T is the total strand concentration, and R is the gas constant. Experimental data were plotted according to the equation above and then were fitted to a straight line by linear regression. Values for ΔH° and ΔS° were estimated from the of slope and intercept, respectively, of the resulting straight line. A window of ±2.25°C was used for calculating the derivative.

CD Studies. CD spectra were recorded on a Jasco (Easton, MD) J500A spectropolarimeter interfaced to a microcomputer. A cylindrical cell with a 10-mm path length was used and the sample temperature was controlled by a Fisher 9000 circulating water bath. The KCl and NaCl titrations were carried out at 20°C. Spectra reported are averages of four scans.

Capillary Electrophoresis. Capillary electrophoresis experiments were carried out at 20°C on a Beckman P/ACE system 2000 operated in the reverse polarity mode, with detection by UV absorbance at 254 nm. All experiments were done at 20°C. A fused silica capillary 37 cm long with a 100-μm inner diameter and a surface coating 0.1 μm thick (DB-17, J & W Scientific, Rancho Cordova, CA) was used. Before each experiment the capillary was rinsed with several column volumes of H_2O. To enhance the separation between the different species, the electrophoresis was done in the presence of a neutral polymer sieving agent, hydroxypropyl methylcellulose (HPMC 4000cp), dissolved in the electrophoresis buffer (0.9%). The buffer containing the polymer was injected under high pressure for 20 min followed by a low-pressure injection of the sample solution for ≈1 min. Electrophoresis was then carried out at constant voltage (7 kV) with data collection at a rate of 1 or 2 Hz. All electrophoresis experiments were performed in buffer containing 25 mM Tris borate, 0.9% HPMC, and the appropriate concentration of KCl or NaCl; sample concentrations were 10–15 μM in strand. The oligodeoxynucleotide $d(T_{10})$ was used in all experiments as an internal marker.

Analytical Ultracentrifugation. Sedimentation equilibrium centrifugation experiments were carried out in a Beckman XL-A analytical ultracentrifuge equipped with absorbance optics. Samples were loaded into a six-channel equilibrium cell with charcoal-filled Epon centerpieces and sedimented at 20°C to equilibrium at 40,000 rpm. The partial specific volume was assumed to be unchanged for all associated oligonucleotide species. The sedimentation equilibrium data for $d(G_3T_4G_3)$ were analyzed as a single ideal species. The absorbance A_r at any radial position r is related to the buoyant molecular weight M_b by the expression:

$$A_r = A_{base} + A_{r_0}\exp\{[\omega^2 M_b(r^2 - r_0^2)]/2RT\},$$

where A_{base} is the baseline absorbance arising from optical artifacts, A_{r_0} is the absorbance at a radial reference distance r_0, ω is the angular velocity, R the gas constant, and T the absolute temperature. The reference radial distance r_0 was set to a radial position two-thirds of the column height. Data were fitted to this equation by nonlinear regression.

NMR Studies. NMR experiments were carried out on a 500-MHz General Electric GN-500 spectrometer equipped with an Oxford Instruments magnet and a Nicolet 1280 computer. Solvent suppression was achieved with a $1\bar{3}\bar{1}$ pulse sequence while recording the proton NMR spectra of samples in 85% H_2O/15% ^2H_2O. A pulse repetition time of 5 s and interval delay of 109 μs were used.

RESULTS

Absorbance Spectroscopy. The UV absorbance spectrum of $d(G_3T_4G_3)$ undergoes a hypochromic change below 285 nm and a hyperchromic shift above 285 nm in the presence of KCl or NaCl (data not shown). A single isosbestic point, present at 285 nm during the titration, suggests the presence of only two species during the titration. The change in absorbance due to addition of KCl appears to be complete by 100 mM KCl whereas that induced by NaCl is complete by 125 mM NaCl.

UV melting analysis of $d(G_3T_4G_3)$ in the presence of 100 mM KCl or NaCl reveals a cooperative monophasic melting transition around 40 or 30°C, respectively. Fig. 1*A* shows the first derivative plots of the melting profiles. In the absence of KCl, no melting transition could be seen. It is also evident that the melting temperature increases with increasing oligonucleotide concentration. Self association in the presence of monovalent cations through quadruplex formation has been reported for similar sequences with G-rich repeats (13–18).

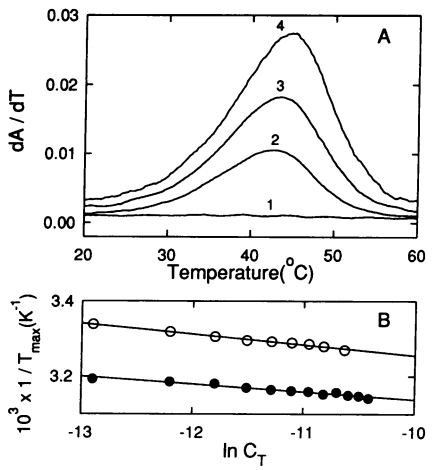

FIG. 1. (*A*) First derivative plot of the thermal melting profiles of $d(G_3T_4G_3)$ in 10 mM Tris·HCl and 0 mM (curve 1) and 100 mM (curves 2–4) KCl. The oligonucleotide concentrations are as follows: Curves: 1 and 2, 10 μM; 3, 17.5 μM; 4, 27.5 μM. (*B*) Plot of ln C_T vs. $1/T_{max}$ for $d(G_3T_4G_3)$ in 10 mM Tris·HCl and either 100 mM NaCl (○) or 100 mM KCl (●).

The difference in the melting temperature for the two systems is consistent with the previous observations that K^+ is a better stabilizing cation than Na^+ for quadruplex structures (4, 6, 17).

Thermodynamic Analysis. The thermodynamics of quadruplex formation were determined from the concentration dependence of the thermal denaturation of $d(G_3T_4G_3)$ in presence of salt, as described above. Fig. 1*B* shows a plot of $1/T_{max}$ against ln C_T, where C_T is the total strand concentration. The linear decrease of $1/T_{max}$ with increasing values of ln C_T indicates that the molecularity of the quadruplex species formed by $d(G_3T_4G_3)$ is >1. The thermodynamic parameters resulting from these experiments (per mol of dimer), are as follows: $\Delta H^\circ = -96.5 \pm 6$ kcal (1 cal = 4.184 J), $\Delta S^\circ = -283 \pm 20$ cal/deg, and ΔG°(at 25°C) $= -11.9 \pm 0.4$ kcal in 100 mM KCl and -69.5 ± 3 kcal, -207 ± 10 cal/deg, and -7.7 ± 0.3 kcal, respectively, in 100 mM NaCl. The values for these parameters in the case of KCl, per guanine quartet, are in qualitative agreement with those reported for four-stranded quadruplexes by Jin *et al.* (16), although these latter were measured in 1 M NaCl.

CD. Fig. 2 shows that formation of the KCl-induced quadruplex in $d(G_3T_4G_3)$ is accompanied by the appearance of a strong positive peak in the CD spectrum at 290 nm. The presence of a peak at 290 nm in these spectra is similar to that reported for other sequences that can exhibit a quadruplex-like structure under certain conditions (16). The spectral changes were complete by 100 mM KCl. Similar results were observed for NaCl, except that complete conversion of the spectrum required 125 mM NaCl (data not shown).

Electrophoresis. A preliminary electrophoresis experiment on $d(G_3T_4G_3)$ in the presence of 100 mM KCl on nondenaturing polyacrylamide gels revealed that the oligomer migrates faster than other single-stranded oligodeoxynucleotides, such as $d(T_{10})$ and $d(C_3T_4C_3)$ (data not shown). We extended these studies using capillary electrophoresis as a faster more convenient technique. Fig. 3 shows the electropherogram for $d(G_3T_4G_3)$ in the presence of increasing concentrations of KCl. Since the migration time for all species changes when the salt concentration changes, a marker, $d(T_{10})$, was used in these experiments and the figure displays the migration time of various species with respect to that of the marker, which has been arbitrarily set to 19 min. It can be seen from the figure that, in the absence of KCl, the unstructured oligomer migrates a little faster than $d(T_{10})$. Addition of KCl results in the appearance of a new peak that migrates even faster. As the concentration of KCl is increased, the intensity of this peak increases with a corresponding decrease in the intensity of the peak for the single-stranded species. At ≈100 mM KCl, the peak corresponding to the single-stranded species disappears completely. In solutions containing 100 mM or more KCl, the faster moving species of $d(G_3T_4G_3)$ migrated as a single sharp peak. It can also be seen from the figure that as the concentration of salt

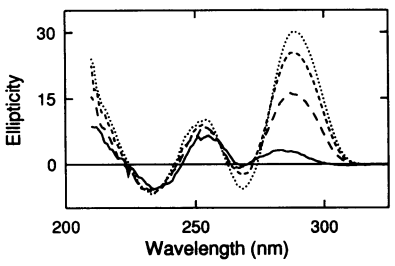

FIG. 2. CD spectra of $d(G_3T_4G_3)$ (15 μM) at 20°C in 10 mM Tris·HCl and in the presence of 0 mM (——), 25 mM (– – –), 50 mM (- - - -), and 100 mM (· · · ·) KCl. Ellipiticity is expressed in millidegrees.

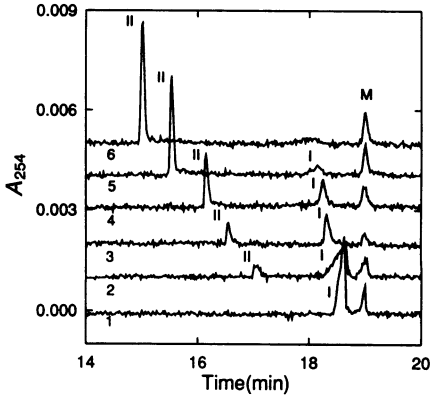

FIG. 3. Capillary electrophoresis traces of $d(G_3T_4G_3)$ at 20°C in the presence of 25 mM Tris borate and various concentrations of KCl. In traces 1–6, KCl concentrations were 0, 5, 15, 25, 50, and 75 mM, respectively. Experiments were carried out at a constant voltage of 7 kV. M, position of the marker; I and II, single-stranded and quadruplex forms of $d(G_3T_4G_3)$, respectively. The traces have been displaced along the vertical axis to facilitate viewing.

is increased, there is an increase in the separation between the two species and between the marker and the two species. Similar results were observed upon addition of NaCl.

Analytical Ultracentrifugation. Equilibrium sedimentation experiments were run on the unstructured oligonucleotide as well as both K^+- and Na^+-induced quadruplex structures, and results are presented in Fig. 4. In the presence of Tris alone, the resultant buoyant molecular weight was observed to be 1492 (average of two values, 1459 and 1525 at 3 and 5 μM strand concentration, respectively). For samples in 200 mM KCl, the oligonucleotide concentrations were 3, 5, 8, and 100 μM in strand, and the resulting buoyant molecular weights were 3150, 3026, 2944, 3059, respectively, with an average of 3045. Although we have not measured partial specific volumes for these samples, we may estimate a

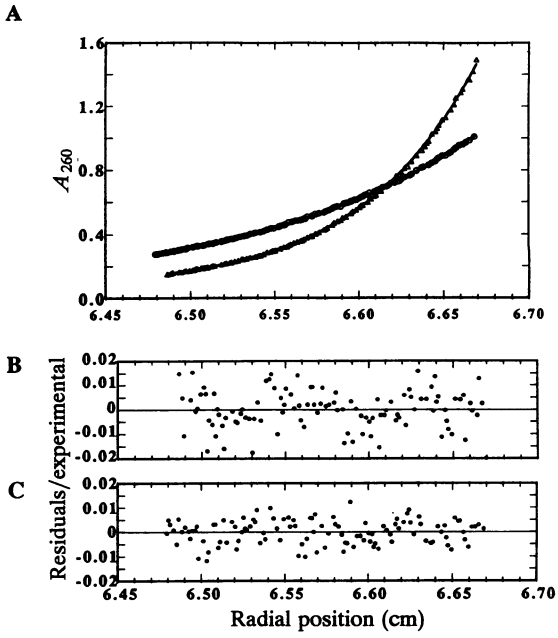

FIG. 4. (*A*) Equilibrium sedimentation results at 20°C for $d(G_3T_4G_3)$ in 200 mM Tris alone (○) and in 10 mM Tris plus 200 mM KCl (△). The smooth line is the best fit to data points by the single-species equation. Resulting buoyant molecular weights are 1492 and 3045 in the absence and presence, respectively, of KCl. (*B* and *C*) Fractional residuals corresponding to Tris plus KCl and to Tris alone, respectively.

molecular weight using a typical value of 0.55 ml/g (24), along with a solution density of 1.005 g/ml. The results are molecular weights of 3336 for the unstructured strand and 6808 for the KCl-induced quadruplex. These results clearly demonstrate that the quadruplex molecular weight is very close to twice that of the unstructured strand, demonstrating that this structure represents a dimer. Also, there is no apparent trend of increasing molecular weight with increasing oligonucleotide concentration, which suggests no tendency to associate into higher-order structures.

Experiments in NaCl were carried out only at 3 μM strand concentration, with a somewhat lower molecular weight of 5983 (average of two runs, 5727 and 6236). This lower molecular weight may be due to the lower thermal stability of the NaCl-induced quadruplex that at 20°C may exist as a mixture of one- and two-stranded forms.

NMR Studies. The addition of salt resulted in dramatic changes in the NMR spectrum of d($G_3T_4G_3$). Fig. 5 displays the NMR spectra of this oligonucleotide in the absence of any salt and in the presence of KCl or NaCl. The exchangeable proton region does not show any resonances in the presence of Tris alone. But on addition of KCl or NaCl, a number of well-resolved sharp resonances appears between 10.9 and 12.1 ppm. These resonances belong to the hydrogen-bonded imino protons formed in the presence of KCl or NaCl, according to the guanine quartet structure displayed in Fig. 6. These new exchangeable proton resonances disappeared on increasing the temperature above 60°C. Decreasing the temperature to 2°C results in the appearance of two broad resonances between 9 and 10.5 ppm. For NaCl, the 10.5 ppm resonance could be seen even at 20°C. These peaks probably arise from thymine imino protons in the loop region.

Fig. 5 also presents the aromatic proton region of the NMR spectra that shows a doubling of peaks upon addition of KCl or NaCl. The KCl-induced changes in the NMR spectrum were complete as the KCl concentration reached 25 mM; further addition of KCl led to significant line broadening. A somewhat higher NaCl concentration (50 mM) was found to be necessary to achieve completion. It is evident that the resonances in the imino and the aromatic regions are more dispersed in the presence of NaCl compared to KCl. In the methyl region, addition of KCl leads to a doubling of all four peaks, whereas in the presence of NaCl, only some of the methyl peaks appear doubled (data not shown).

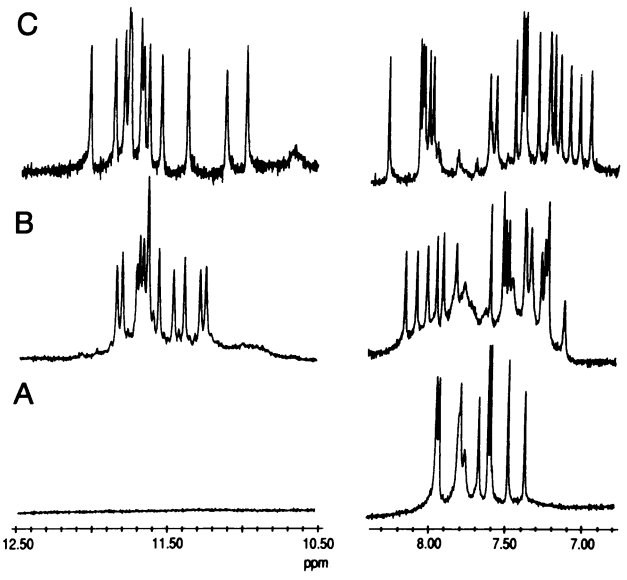

FIG. 5. ^{1}H NMR spectra at 500 MHz of d($G_3T_4G_3$) in 10 mM Tris·HCl alone (*A*) and in 10 mM Tris·HCl plus 25 mM KCl (*B*) or 70 mM NaCl (*C*). The spectra were recorded at 20°C. Concentration of the samples (in strand) was 3 mM for *A* and *B* and 1.6 mM for *C*. Imino proton regions in *A* are from spectra obtained in 85% H_2O/15% ^2H_2O, and aromatic regions in *B* and *C* were recorded in ^2H_2O.

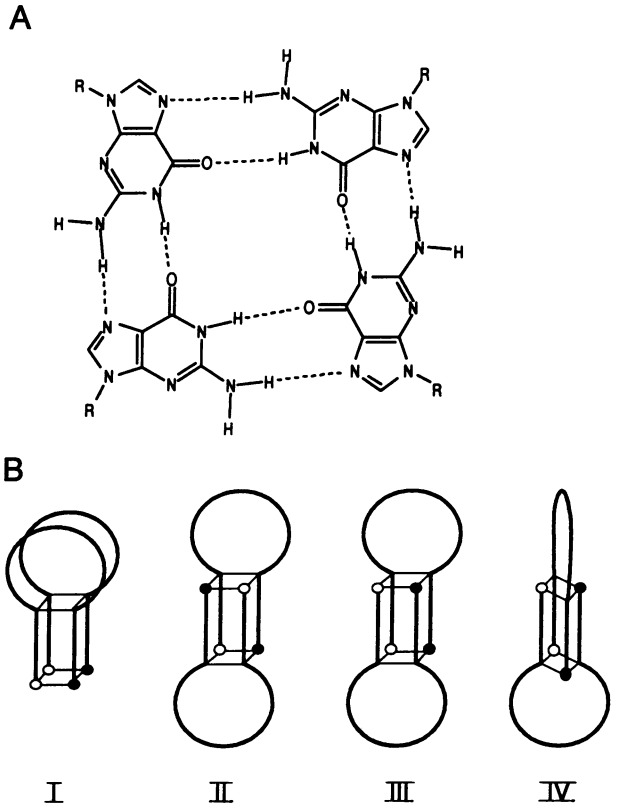

FIG. 6. (*A*) Hydrogen bonding scheme for a guanine quartet. (*B*) Schematic representation of possible asymmetric (structures I and II) and symmetric (structures III and IV) hairpin dimer structures. In each of these structures, the 3′ and 5′ ends are represented by open and solid circles, respectively. Structure I is asymmetric due to the lack of symmetry in the guanine quartet, shown in *A*, and structure II can be asymmetric due to the arrangement of the nucleoside conformations about the glycosidic bond. Structures III and IV each possess a C_2 axis of symmetry.

DISCUSSION

Several synthetic oligonucleotides with guanine-rich repeats have been shown to form single- or multistranded structures involving guanine quartets stabilized by Hoogsteen-like hydrogen bonding. Though there have been a few studies aimed at the physicochemical and structural characterization of quadruplex structures formed by relatively short sequences, few generalizations can be made at this time concerning the relation of sequence to tertiary structure or the role of different cations in stabilizing various conformations. Results from experiments described above clearly demonstrate that d($G_3T_4G_3$) acquires a folded structure in the presence of KCl or NaCl and is consistent with quadruplex formation.

The capillary electrophoresis results described here demonstrate the utility of this technique in the study of DNA secondary and tertiary structure. The electropherograms presented in Fig. 3 clearly show the formation of the new species at the expense of the single-stranded form on addition of KCl. The electrophoresis was done in a capillary coated on the inside to eliminate electroosmotic flow and filled with a neutral polymer sieving agent. Under these experimental conditions, one may expect smaller or very compact molecules to migrate faster than large molecules. The quadruplex structure formed in the presence of KCl or NaCl has a substantially greater electrophoretic mobility than that of the

single-stranded species, suggesting the very compact nature of the structure.

The $d(G_3T_4G_3)$ sequence can potentially form a quadruplex either by the association of four strands stabilized by six guanine quartets or by the association of two hairpins stabilized by three quartets. The latter model is expected to be more compact and the electrophoresis results support this model for $d(G_3T_4G_3)$ in the presence of KCl or NaCl. The capillary electrophoresis experiments provide evidence that a single compact species is formed, at least at optical concentrations. More definitive evidence of the dimer structure is obtained from ultracentrifugation experiments. It is clear from our data that the buoyant molecular weight of the quadruplex is equivalent to two strands of $d(G_3T_4G_3)$ and, hence, represents a two-stranded rather than a four-stranded structure. We have not measured the partial specific volumes, which may be different for the unstructured and quadruplex species. They may also differ in molecular weight due to differences in bound cations. For these reasons, accurate masses are not yet available. Nonetheless, the evidence in favor of a two-stranded structure is very strong.

The proton NMR spectrum of $d(G_3T_4G_3)$ in H_2O in the presence of Tris alone does not shown any resonances in the exchangeable proton region, whereas the aromatic and methyl proton regions show 10 and 4 resonances, respectively, as expected for $d(G_3T_4G_3)$ in an unstructured conformation. But in the presence of KCl or NaCl, the exchangeable proton region shows 12 well-resolved sharp resonances between 10.9 and 12.1 ppm due to the hydrogen-bonded guanine imino protons. A single guanine quartet will have four imino protons engaged in Hoogsteen-type hydrogen bonding. Based on this, the 12 imino resonances in the presence of salt indicate that these protons are magnetically nonequivalent, implying that the underlying structure is asymmetric. The aromatic proton region shows a doubling of the number of resonances on the addition of salt, again indicating the lack of symmetry. The sharpness of the resonances is expected for a compact dimer species. Preliminary two-dimensional NMR experiments indicate that half of the guanines are in the *syn* conformation, consistent with previous reports (18–21).

Although all of our data strongly support a single asymmetric dimer, it is possible that the system is composed of two symmetric dimers with different NMR chemical shifts but behaves identically in all other experiments. We feel this is highly unlikely, since NMR spectra recorded at different temperatures showed no change in the relative intensities of the various resonances.

Having established the molecularity of the complex, we were able to determine the thermodynamic parameters for formation of the quadruplex structure from the concentration dependence of the melting temperature. The results provide a quantitative indication of the greater stability of the KCl-induced structure compared to the NaCl-induced form. Even though $d(G_3T_4G_3)$ exists as a hairpin dimer in the presence of KCl and NaCl, there are some obvious differences in their NMR spectra. This may be due to differences in the geometry and orientation of the bases when bound to these cations, rather than any major topological differences.

The fact that both K^+ and Na^+ stabilize hairpin dimer structures is of interest in light of evidence for a Na–K switch governing the molecularity of quadruplex structures. Sen and Gilbert (6) have shown that several telomeric sequences can form four-stranded structures in the presence of Na^+ but prefer more compact foldback structures in the presence of K^+. It appears that the overall molecularity of the structure formed by $d(G_3T_4G_3)$ is the same in both Na^+ and K^+. It is of interest to note that a closely related sequence, $d(G_2T_5G_2)$, has been reported to form a four-stranded quadruplex in the presence of Na^+ (16). It is apparent that sequence plays a major role in determining the overall structure in these systems.

One important feature common to both salt-induced structures of $d(G_3T_4G_3)$ is their asymmetry. Some of the possible arrangements of two hairpins are presented in Fig. 6*B*, of which structures I and II are asymmetric. This is of particular interest in light of the recent reports (20, 21) on the solution and crystal structure of a closely related sequence, $d(G_4T_4G_4)$. Whereas both of those structures were observed to be symmetric, they are different in their topology. Thus, the x-ray crystal structure of $d(G_4T_4G_4)$ reveals a symmetric dimeric hairpin as shown in Fig. 6*B*, structure III, and the symmetric NMR structure resembles that shown in Fig. 6*B*, structure IV. With the asymmetric conformations illustrated in Fig. 6*B*, structures I and II, it is apparent that these G-rich sequences can assume a wide variety of structures. One major goal of future work should be to understand the role of sequence and cations in determining which of the many forms is the most stable.

We are grateful to Dr. Corey Levenson, Cetus Corp., for providing the $d(G_3T_4G_3)$ oligonucleotide; Ms. K. J. Ulfelder, Beckman Instruments, for extensive discussions on the design of capillary electrophoresis experiments; and Ms. K. Turner of J & W Scientific for generously providing capillaries for our initial studies. This work was supported by grants from the National Cancer Institute (CA 27343), and the University of California Systemwide Biotechnology Research and Education Program. We also acknowledge the National Cancer Institute for the purchase of the Beckman P/ACE 2000 capillary electrophoresis instrument through Grant 1 S15 CA 53726-01.

1. Blackburn, E. H. & Szostak, J. W. (1984) *Annu. Rev. Biochem.* **53**, 163–194.
2. Zakian, V. A. (1989) *Annu. Rev. Genet.* **23**, 579–604.
3. Blackburn, E. H. (1990) *J. Biol. Chem.* **265**, 5919–5921.
4. Sundquist, W. I. & Klug, A. (1989) *Nature (London)* **342**, 825–829.
5. Hastie, N. D. & Allshire, R. C. (1989) *Trends Genet.* **5**, 326–331.
6. Sen, D. & Gilbert, W. (1990) *Nature (London)* **344**, 410–414.
7. Sen, D. & Gilbert, W. (1988) *Nature (London)* **334**, 364–366.
8. Evans, T., Schon, E., Gora-Maslak, G., Patterson, J. & Efstratiadis, A. (1984) *Nucleic Acids Res.* **12**, 8043–8058.
9. Kilpatric, M. W., Torri, A., Kang, D. S., Engler, J. A. & Wells, R. D. (1986) *J. Biol. Chem.* **261**, 11350–11354.
10. Gellert, M., Lipsett, M. N. & Davies, D. R. (1962) *Proc. Natl. Acad. Sci. USA* **48**, 2013–2018.
11. Lipanov, A. A., Quintana, J. & Dickerson, R. E. (1990) *J. Biomol. Struct. Dynam.* **8**, 483–489.
12. Zimmerman, S. B., Cohen, G. H. & Davies, D. R. (1975) *J. Mol. Biol.* **92**, 181–192.
13. Williamson, J. R., Raghuraman, M. K. & Cech, T. R. (1989) *Cell* **59**, 871–880.
14. Panyutin, I. G., Kovalsky, O. I., Budowsky, E. I., Dickerson, R. E., Rikhirev, M. E. & Lipanov, A. A. (1990) *Proc. Natl. Acad. Sci. USA* **87**, 867–870.
15. Henderson, E., Hardin, C. C., Walk, S. K., Tinoco, I., Jr., & Blackburn, E. H. (1987) *Cell* **51**, 899–908.
16. Jin, R., Breslauer, K. J., Jones, R. A. & Gaffney, B. L. (1990) *Science* **250**, 543–546.
17. Hardin, C. C., Henderson, E., Watson, T. & Prosser, J. K. (1991) *Biochemistry* **30**, 4460–4472.
18. Wang, Y., de los Santos, C., Gao, X., Greene, K., Live, D. & Patel, D. J. (1991) *J. Mol. Biol.* **222**, 819–832.
19. Wang, Y., Jin, R., Gaffney, B., Jones, R. A. & Breslauer, K. J. (1991) *Nucleic Acids Res.* **19**, 4619–4622.
20. Kang, C., Zhang, X., Ratliff, R., Moyzis, R. & Rich, A. (1992) *Nature (London)* **356**, 126–131.
21. Smith, F. W. & Feigon, J. (1992) *Nature (London)* **356**, 164–168.
22. Griswold, B. L., Humoller, F. L. & McIntyre, A. R. (1951) *Anal. Chem.* **23**, 192–194.
23. Gralla, J. & Crothers, D. M. (1973) *J. Mol. Biol.* **78**, 301–319.
24. Bloomfield, V. A., Crothers, D. M. & Tinoco, I., Jr. (1974) *Physical Chemistry of Nucleic Acids* (Harper & Row, New York).